*Egyptian Geophysical Society*
*EGS Journal, Vol. 22, No. 1, 47-63 (2024)*

# Challenges of Lateral Transfer Pore Pressure Mechanism and its Impact on Non-Productive Time Deep water, Nile Delta, Egypt

Ahmed I. Abushady[1]*, Abdel-Khalek M. EL-Werr[2], Nasser M. Abou Ashour[2]
[1] Department of Global Subsurface Solutions, British Petroleum (BP), Cairo, Egypt
[2]Department of Geophysics, College of Science, University of Ain shams, Cairo, Egypt
* **Corresponding Author**: Ahmed I. Abushady: aaifbn@uk.bp.com
British Petroleum (BP), Cairo Festival City, Business Park D, Plot #14 D03, Cairo 11477, Egypt.

**Abstract**

Typically, the level of uncertainty in pore pressure would decrease for development wells that are drilled 400-900 meters apart after an exploratory discovery. In contrast to expectations, the uncertainty in pore pressure has not decreased for development wells drilled in the Raven field of the West Nile Delta offshore deep-water basin. Pore pressure related problems were attributed to differences in lateral pressure transfer mechanism in relatively thin and isolated sand units of Lower Serravallian epoch (Sidi Salim FM) along the study area. Authors bringing something fresh and original to the table of pore pressure that has not been done before within Nile Delta. Rapid sedimentation rate in the deep water of West Nile Delta basin in Egypt is one of the primary causes for the development of overpressure systems. In this setting, pore fluids unable to escape naturally during deposition. This study introduced other mechanism contribute to the overpressure zones, which is ignored while planning. The main purpose of this study is to investigate the impact of lateral transfer pore pressure mechanism on the differentiation between the shale and sand pore pressures and how to mitigate the associated kick /influx problems. Authors articulated best workflow and recommendations to minimize miss interpretation and risk of repeated non-productive time of studied wells. Shale pore pressure was derived from seismic, sonic and resistivity logs. Furthermore, 3D seismic volume used to estimate sand relief and finally sand lateral transfer pore pressure were estimated using centroid calculations methods.

**Keywords:** Lateral Transfer, Nile Delta, Pore Pressure, Influx, Non-Productive Time.

## 1. Introduction

The poorly understood lateral transfer overpressure mechanism was one of the main causes of well control problems (kick/influx) that resulted in non-productive time in Raven development wells. This study investigated key reasons for over-pressured sands recorded in some wells and how to mitigate this in future well planning and execution. Recent drilling of four development wells in the Raven field identified heterogeneity in both sand distribution and pore pressure within the Lower Serravallian sandstone. The studied wells were drilled in the eastern segment of the field very close to each other and experienced significantly different pore pressure. This study structure was built on detailed analysis of the well logs, drilling problems, and seismic-derived pore pressure to demonstrate the challenges of predicting lateral transfer pressure in thin sand units below seismic resolution. High formation pressure exceeding normal hydrostatic pressure is termed overpressure (Dutta 1987). High formation pressure is typically found in young, rapidly deposited clastic rocks (primarily sandstone, shale, and siltstone) because of incomplete dewatering of fine-grained rock, such as shale, which is known as compaction disequilibrium (Mouchet and Mitchell, 1989; Chapman, 1994 and Osborne and Swarbrick, 1997). This process indicates that the more shale exists in the sedimentary succession, the greater the likelihood of high pressure.

The amount of overpressure is a function of the permeability of the rock (how fast the water can escape when the formation is buried) and the rate of burial. However, there are other reasons for high pressure primarily related to deeper processes occurring in the rock column at elevated temperatures. It follows from the previous description of the mechanisms that three primary components control where overpressure occurs - rate of sediment burial, temperature, and sediment permeability. The literature has checked several methods to predict over pressured intervals pre-drill using seismic velocity data (see Eaton 1975; Heppard and Albertin 1998; Sundaram and Jain 2008; Babu and Sircar 2011; Brahma et al. 2013; Karthikeyan et al. 2018; Das and Soumyajit M 2020). The best method gave best shale pore pressure results was mainly Eaton and Presgraph which is later integrated with lateral transfer pore pressure calculation.

The concept of the centroid was described by Traugott (1997) and has also been referred to as “lateral pressure transfer” (Yardley and Swarbrick, 2001). The concept assumes that there is a midpoint (the “centroid”) along a dipping sequence of permeable reservoirs and sealing non-reservoirs, where the pore pressure is in pressure equilibrium. At this point, the predicted pore pressure in the sealing non-reservoir is assumed to be equal to the pore pressure in the porous reservoir. The overpressure at this point will be transferred throughout the full extent of the porous reservoir interval. Therefore, as each of the wells may connect into a different water bearing channel, which has a different downdip extent, and therefore different overpressure associated with lateral transfer of pressure, the pore pressures encountered may be quite variable. In this case study, it is observed that the simple use of offset well data as the analog in forecasting pore pressure would give erroneous results. Careful analysis and interpretation of 3D seismic data over sandy intervals is critical for potential pre-drill detection of intervals with lateral transfer overpressure risk. The Raven field study area lies within the west Nile Delta basin, in a water depth of approximately 650 m below sea level, 40 km north of Alexandria. The Rosetta canyon divides the study area into a western and eastern sides, both of which are located within the north Alexandria concession, Offshore Egypt (Fig.1).


(1a)

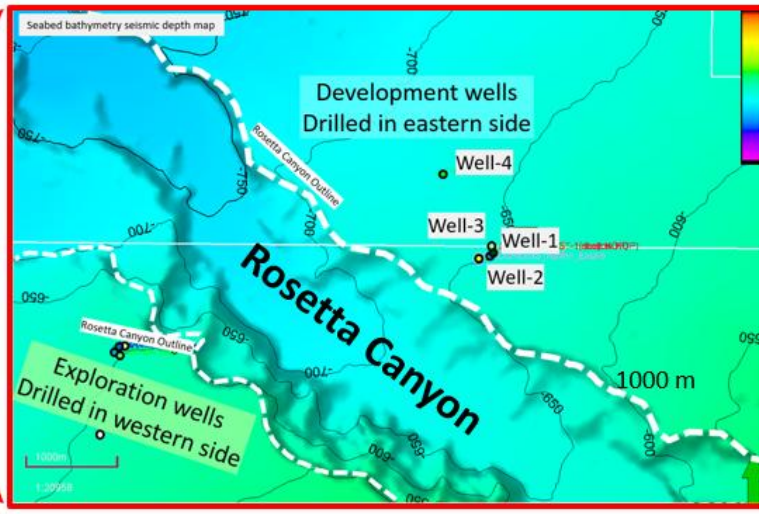


(1b)

**Fig. 1. (a) Study area location map; north Alexandria concession includes Raven filed. (b) Rosetta canyon divides the study area into a western and eastern sides.**

In the early discovery and appraisal wells for Raven that drilled on the west side of the field, there were no significant sands encountered in the Lower Serravallian (Sidi Salim Formation) interval. However, the recent development drilling in 2016 on the east side encountered a channel complex. In the first two wells, there were no major problems, and the measured sand pressure was equivalent to 15 ppg. However, in the third well, the sand pressure was high enough to result in an influx equivalent to 15.5 ppg, then a geologic sidetrack and an additional casing string. In the fourth well, the casing design was changed to add the additional casing string to mitigate problems associated with higher sand pressures equivalent to 15.7 ppg. The stress state in the Nile Delta area of interest is interpreted to be extensional in nature, with the post-Messinian sedimentary sequence 'sliding down' into the Mediterranean basin on the near flat-lying Messinain evaporitic sequence, resulting in extensional faulting above the Messinian Anhydritic limestone No salt diapirs, or associated stress rotations, are observed in the study area (Maha et al., 2022).

This study aims to investigate the impact of lateral transfer pore pressure mechanism on the differentiation between the shale and sand pore pressures and how to mitigate the associated kick /influx problems. Authors articulated new workflow and recommendations to minimize miss interpretation and risk of repeated non-productive time of studied wells. Shale pore pressure was derived from seismic, sonic and resistivity logs. Furthermore, 3D seismic volume used to estimate sand relief and finally sand lateral transfer pore pressure were estimated using centroid calculations methods.

**2. Geologic and stratigraphic setting**

Stratigraphic framework of the Nile Delta has been built out into the Mediterranean by the present and ancestral Nile River, both as high-stand siliciclastic coastal deposits and low-stand deep sea fans from shelf bypass. A major desiccation event in the Messinian (Upper Miocene) was followed by a major Pliocene transgression reaching far inland and most exploration to date, in the West Nile Delta, has been for biogenic gas in Pliocene channel deposits (Ismail et al., 2020 and 2022). A simplified stratigraphic column identifying drilled stratigraphic sequences and highlighting the problematic sand bodies of Serravallian sands (Fig.2). Middle Miocene Serravallian sands (problematic zone) of Sidi Salem FM, that observed in most of the drilled wells with variable pore pressure magnitudes. The entire Tortonian/Messinian succession has been eroded by compound unconformities (Kellner et al. 2018). The Late Serravallian to Early Tortonian is mainly characterized by a sand/shale section of fluvial channel systems across the field. The E1 and E3 wells, that drilled west of Rosetta canyon, had pore pressures (PP) of approx. 15 ppg equivalent mud weight (EMWT) and Wells 1, 2, 3 and 4, east of the Rosetta canyon, had even higher PP of approx.15.7 ppg EMWT.

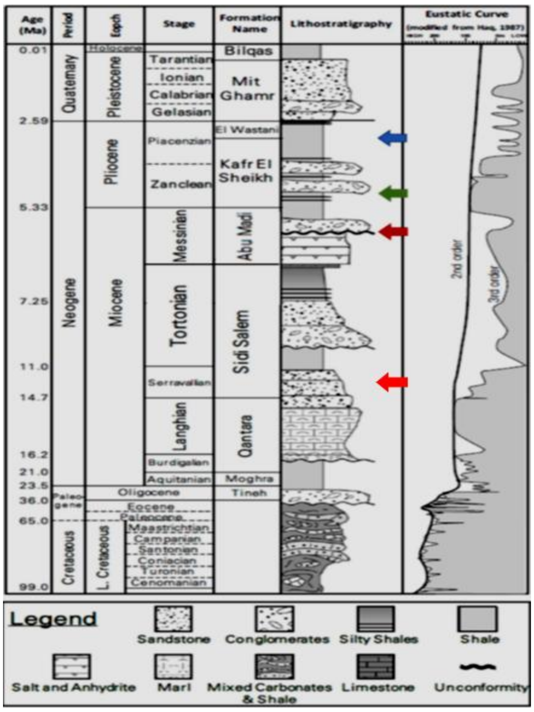


**Fig. 2. Stratigraphy of the Nile Delta (modified after Saleh 2018), where the blue, green and red arrows refer to the three expected overpressure intervals in study area.**

The structural pattern of the Nile delta is the result of a complex interplay between three main fault trends. The first is the NW-SE oriented Misfaq-Bardawil (Temsah) fault trend, the second is the NE-SW oriented Qattara-Eratosthenes (Rosetta) fault trend (Neev, 1975; Argyriadis, et al., 1980 and Abdel Aal, et al., 1994) and the third is the E-W fault trend delineating the Messinian salt basin. These trends are parallel to the Circum-Mediterranean plate boundaries and seem to be old inherited basement faults, which reactivate periodically throughout the development of the area (Fig.3).

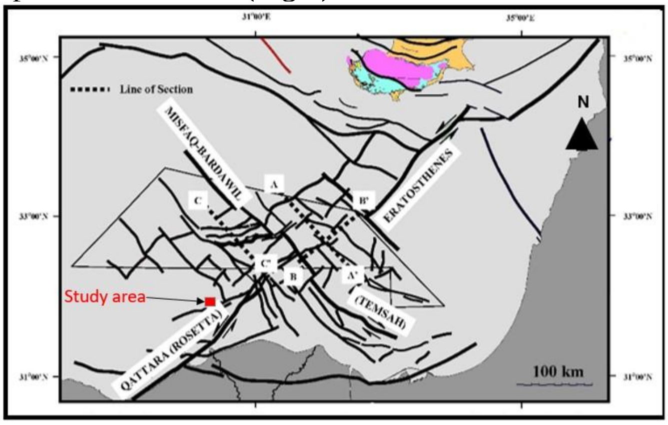


**Fig. 3. Mediterranean structure map, showing the main NE-SW (Qattara-Eratosthenes) left to lateral oblique-slip, NW-SE (Misfaq-Bardawil) right-lateral oblique-slip and E-W gravitational normal faults trends (modified after Abdel Aal, et al., 2000).**

## 3. Dataset and methods

Formation pore pressure can be determined by either direct or indirect methods (Lesso and Burgess 1986). The direct pressure measurements provide promising results in permeable formations, where the measurement tool is placed along the formation and allows sufficient time to reach pressure equilibrium. However, pore pressure in very low permeability formations such as shale, cannot be measured by direct measurements. This study flowchart (Fig.4) was considered predrill and post drill data from four wells, these wells were drilled recently by British Petroleum (BP) company. Available logs including sonic and Resistivity, and the seismic interval velocity were used to indirectly estimate the shale pore pressure. Sand pore pressure was derived from direct pressure measurements and inferred from kick events of the problematic wells, also up dip sand pressure was calculated using centroid equation. Shale and sand pore pressure results were validated to drilling observations and measurements over studied wells. Shale is quite sensitive to compaction process and therefore, it has been used as a key parameter for the determination of pressure profile in sedimentary rocks (Muir 2013). The most popular prediction methods for pore pressure are: (1) The Effective stress, also called Equivalent Depth Method and (2) Eaton's Method (Fig.5). The fundamental concepts for estimating pore pressure in shale formations are the knowledge of overburden stress, effective stress, and the knowledge of porosity dependent parameters (Hower et al. 1976).


**Fig. 4. Recommended workflow to avoid missing the potential for lateral transfer (centroid) of overpressure.**

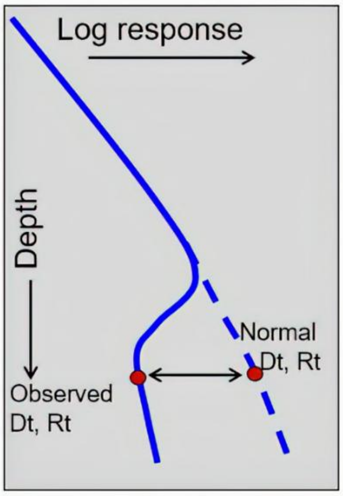


**Fig. 5. A diagram of Eaton's method and the effective stress method (Eaton, 1975).**

Gardner empirical equation 1 was used to predict the pseudo bulk density from seismic interval velocity that was less than the density results predicted from Bellotti and Giacca (1978) Eaton's method was used to estimate shale pore pressure. The principle of Eaton's method is the comparison of the log data and the drilling data with the normal compaction trends (NCTs) at the same depths. Eaton (1975) developed four equations for pore pressure estimation using well logs and drilling data. Among pore pressure estimation methods that use logs data, Eaton's method is the most widely used. In this study, Interval transit time (DT) in (µs⁄ft), which is a porosity-dependent parameter (i.e., increases with increasing porosity) can be calculated from seismic interval velocities in (m / s) across the study area applying the following equation 2 (Hottman and Johnson 1965). The PRESGRAF Amoco overburden, normal compaction trend and pressure transform models, developed by Martin Traugott (Heppard et al. 1998), were used as another tool to predict pore pressure. The Presgraf model is based on a global database and has a generic definition of how rocks are expected to compact with depth.

$$\boldsymbol{\rho b = 0.31 \times V_p\ 0.25} \quad \textbf{(1)}$$

$$\boldsymbol{(DT) in\ (\mu s/ft) = \frac{0.3048 \times 10^6}{V_p}} \quad \textbf{(2)}$$

Where:

$\boldsymbol{\rho b}$ is pseudo-Bulk density in (gm⁄cc),

$\boldsymbol{DT}$ is Observed Acoustic slowness or travel time (Compressional sonic log) in (µs⁄ft), and

$\boldsymbol{V_p}$ is Observed Seismic compressional interval velocity in (ft/sec),

To calculate shale pore pressure equation 3 were used for seismic derived pore pressure, equation 4 for sonic log resistivity derived pore pressure estimation and equation 5 for resistivity log derived pore pressure estimation. The resulting pore pressure are then compared to the in-situ pressure indicators (e.g., Connection Gas (CG), Pump off Gas (POG), pressure caving) or measurements of fluid pressure (MDT) in isolated sands/silts.

$$\boldsymbol{PP = S_V - (S_V - P_{norm}) \times (V_p/V_{p_{trend}})^k} \quad \textbf{(3)}$$

$$\boldsymbol{PP = S_V - (S_V - P_{norm}) \times (DT_O/DT_N)^k} \quad \textbf{(4)}$$

$$\boldsymbol{PP = S_V - (S_V - P_{norm}) \times (R_O/R_N)^k} \quad \textbf{(5)}$$

Where:

$\boldsymbol{PP}$ is Pore Pressure (psi),

$\boldsymbol{S_V}$ is Vertical stresses (Overburden Gradient) (psi),

$\boldsymbol{P_{norm}}$ is Normal Pore pressure (psi),

$\boldsymbol{V_p}$ is Observed Seismic compressional interval velocity in (ft/sec),

$\boldsymbol{V_{p_{trend}}}$ is Seismic compressional interval velocity in (ft/sec) for normally pressured formations,

$\boldsymbol{R_O}$ is Observed Resistivity (ohms-m),

$\boldsymbol{R_N}$ is Normal Resistivity (ohms-m),

$\boldsymbol{DT_O}$ is Observed Acoustic slowness or travel time (Compressional sonic) in (µs⁄ft),

$\boldsymbol{DT_N}$ is Normal PP Acoustic slowness or travel time (Compressional sonic) in (µs⁄ft), and

$\boldsymbol{k}$ is Eaton Exponent (dimensionless), which is, 1.2 in for resistivity and 3 for sonic and seismic.

When discrepancy observed between estimated pore pressure and measured or inferred sand pore pressure, study applied sand lateral transfer pore pressure calculation. Equation 6 was used for sand observed above centroid depth (Up dip sand) and equation 6 were used for sand observed below centroid depth (Down dip sand). Finally convert all pore pressure to equivalent mud weight (EMWT) in ppg as equation 7. Pressure differences are driven by the natural difference in pressure gradients between over pressured shales and sands.

$$\boldsymbol{PP}(\boldsymbol{up\ dip}) = \textbf{Centroid PP} - (\textbf{TVD} \times \boldsymbol{\rho_{fl}}) \quad \textbf{(6)}$$

$$\boldsymbol{PP}(\boldsymbol{down\ dip}) = \textbf{Centroid PP} + (\textbf{TVD} \times \boldsymbol{\rho_{fl}}) \quad \textbf{(7)}$$

$$\boldsymbol{EMWT} = \left(\frac{\boldsymbol{PP(PSI)}}{\boldsymbol{TVD}}\right) \times \mathbf{19.25} \quad \textbf{(8)}$$

Where:

$\boldsymbol{PP}(\boldsymbol{up\ dip})$ is Up dip sand lateral transfer pore pressure (psi),

$\boldsymbol{PP}(\boldsymbol{down\ dip})$ is Down dip sand lateral transfer pore pressure (psi),

**Centroid PP** is Shale pore pressure (Shale PP =Sand PP) (psi),

**TVD** is true vertical depth (ft),

$\boldsymbol{\rho_{fl}}$ is Pore fluid density gradient in (psi/ft), and

$\boldsymbol{EMWT}$ is Equivalent mud weight (EMWT) in (ppg),

## 4. Results

Despite several wells being drilled through these thin sands in the Lower Serravallian epoch only 400-900 meters apart, pore pressure uncertainty was found as the main cause of non-productive time. The drilling of development wells in the study area started in 2015 with Well-1, Well-2, Well-3, and Well-4, respectively, and ended in 2017. The development wells that were drilled on the eastern side of the canyon showed high pressure at the base Serravallian sands that causes a lot of influxes and non-productive time. These problematic sands were not recorded in the exploratory and appraisal wells (E1 and E3 Wells), that were drilled in 2004, on the other hand, this problematic sand deposits were not penetrated by any of the development wells drilled on the western side of the canyon (Fig.6). Although the wells drilled on the eastern side of the canyon are very close to each other at the Serravallian level (400-900 m apart), the measured pore pressure of the influxes is completely different.

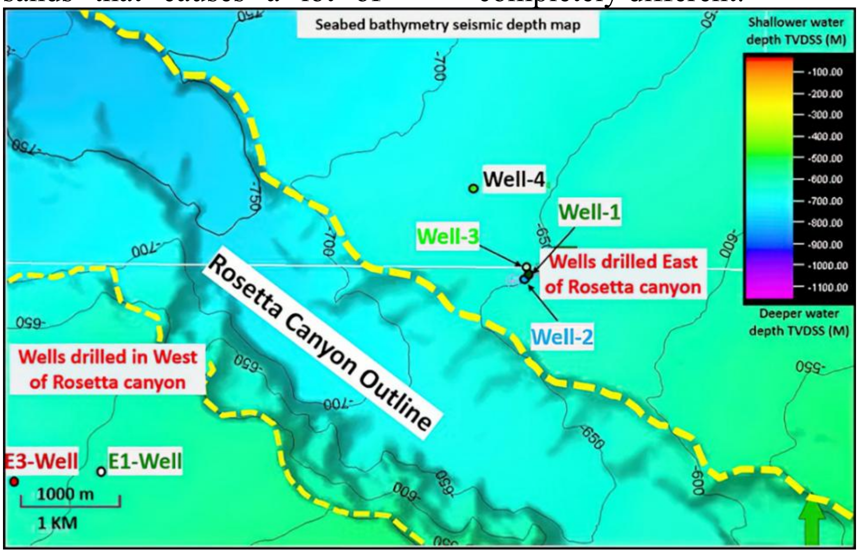


**Fig. 6. Rosetta Canyon divide study area to west and East.**

**4.1.**

**Overpressure detection**

The first well (Well-1) that penetrated a base Serravallian sand, shown in the seismic section in (Fig.7), recorded high connection gases, swabbed influx, and final measured sand-PP of about 15 ppg EMWT. The base Serravallian sand was drilled with a surface mud weight (SMWT) of 14.4 ppg (underbalanced condition) but did not flow either while drilling or on stand-pipe connection. However, the sand was slowly bleeding, and an influx was observed while wireline logging. It took a long time for the sand to flow after a potential swab while pulling out of hole (POOH) with the drilling assembly. A formation pressure test (modular dynamic tester; MDT) was taken from the base Serravallian sand in Well-1, which was interpreted to be 15 ppg (Over pressure=4642 PSI). The pressure was still building very slowly due to the low permeability of the sand. However, an expert petrophysics confirmed that the point could be considered stable. Finally, the influx from the base Serravallian sand was killed in Well-1 with 15.05 ppg SMWT, which equated to an equivalent static density (ESD) from pressure while drilling (PWD) of 15.17 ppg. The sand was found to be water bearing, but with residual gas.

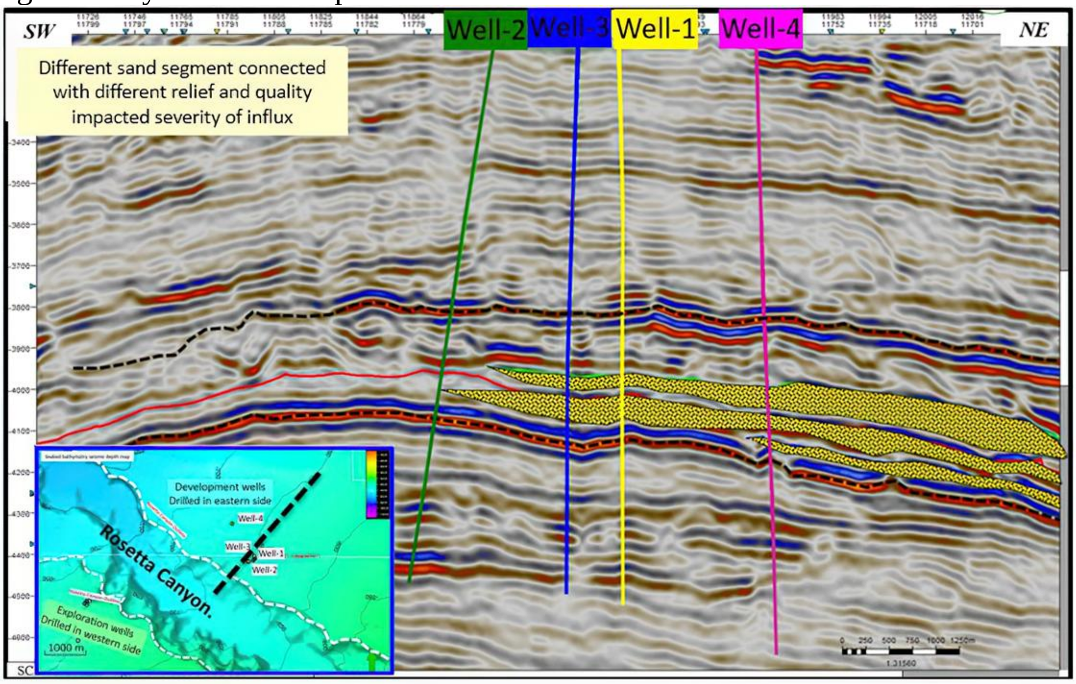


**Fig. 7. SW-NE seismic section across the 4 studied wells confirming different relief and anisotropic quality of sand channels, which grade to shale toward SW at Well-2.**

The second well (Well-2) was drilled 200m away from Well-1 with higher SMWT, compared to first well (Well-1), but no problems were recorded in the same interval that was encountered in well-1. This was interpreted to be the absence of the bleeder sand in well-2 because the sand graded into shale towards the SW as shown in seismic section (Fig.8).

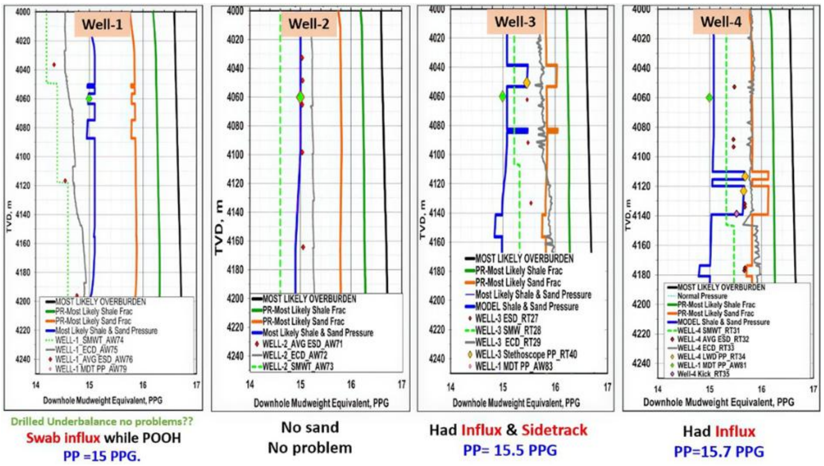


**Fig 8. PPFG correlation showing different pore pressure magnitudes along four wells drilled 400-900m apart, reflecting high heterogeneity and different overpressure mechanisms.**

The third well (Well-3) was drilled 400 m away from Well-1; the subject sand pore pressure was predicted to be 15 ppg based on the MDT measured pressure in the closed offset Well-1. The targeted ESD to drill Well-3 base Serravallian sand was set at 15.1 ppg. Well-3 was sidetracked after it encountered shallow problems. Well-3 ST1 was drilled with 14.75 ppg SMWT, the equivalent static density (ESD) from pressure while drilling (PWD) was 15.17 ppg. The ESD could potentially be reduced to 14.95 ppg based on the vertical hydraulic modeling, if the PWD tool were giving incorrect values. The observed underbalanced indicators were as follows:

1) Connection gases (CG) were recorded while drilling at 4021 m depth level TVDBRT 1.5 % of gas with ESD of 15.15 ppg and at 4061 m depth level 2.2 % of gas with ESD 15.13 ppg, showing and increasing gas trend validating the overpressure sand zone.
2) Influx 3 barrels (bbls) while drilling at 4086 m level.
3) Flow check gained 1.1 bbls in 8 minutes.
4) Shut in well and monitored shut-in casing pressure (SICP), which was 168 psi. The final kill mud weight (KMWT) was 15.05 ppg.

While killing, the well-3 went into losses during the second circulation and was subsequently sidetracked. The sidetrack plan included running an extra casing to cover the weak zones above the base Serravallian (influx) sand, to allow for increasing the MWT above 15.3 ppg (PWD equivalent circulating density (ECD). Well-3 ST managed to drill the influx sand with a surface mud weight of 15.25 ppg, ESD of approximately 15.5 ppg and ECD of 15.78 ppg without any problems. The base Serravallian sand pore pressure was eventually measured to be 15.49 ppg EMWT (Over pressure=4881 PSI) (Fig.9). The fourth well (Well-4) was drilled about 600 m from Well-1 and 800 m from Well-3. It was drilled with slightly higher MWT compared to Well-3ST as shown. It had connection gases followed by a kick while drilling at the same base Serravallian sand that was killed with a MWT of 15.7+ ppg. The measured pressure in Well-4 kick sand was 15.71 ppg EMWT (Over pressure=5125 PSI).

### 4.2 Observations

Limitations of common pore pressure estimation techniques arise when only compaction disequilibrium overpressure generation mechanism and a small-scale seismic volume were considered, neglecting the impact of lateral transfer in highly dipping sand intervals. The difference between pre-drill and post-drill pore pressure prediction was interpreted simply as a deficiency of the common methods if lateral transfer overpressure of highly dipping sands was not considered. Lateral transfer overpressure mechanism simply is the movement of overpressure along dipping, relatively higher permeability intervals to a shallower formation, sometimes referred to as centroids. Sands drilled up dip will have significantly higher pore pressure gradient (e.g., Equivalent Mud Weight in ppg) than sands drilled down dip. Although the overburden pressure (OVP) will be the same throughout the permeable sandstone. There should never be an OVP gradient in a single sandstone body or well-connected sandstone bodies. The greater the relief in the sand, the greater the change in pressure gradient moving from the syncline to the crest. The greater the magnitude of overpressure in the sand, the greater the change in pressure gradient moving from the syncline to the crest (Fig.9a). The overburden difference plays a key factor on lateral transfer overpressure magnitude, as sandstone intervals that dip landward will show a higher overpressure compared to sands that dip seaward (Fig.9b).

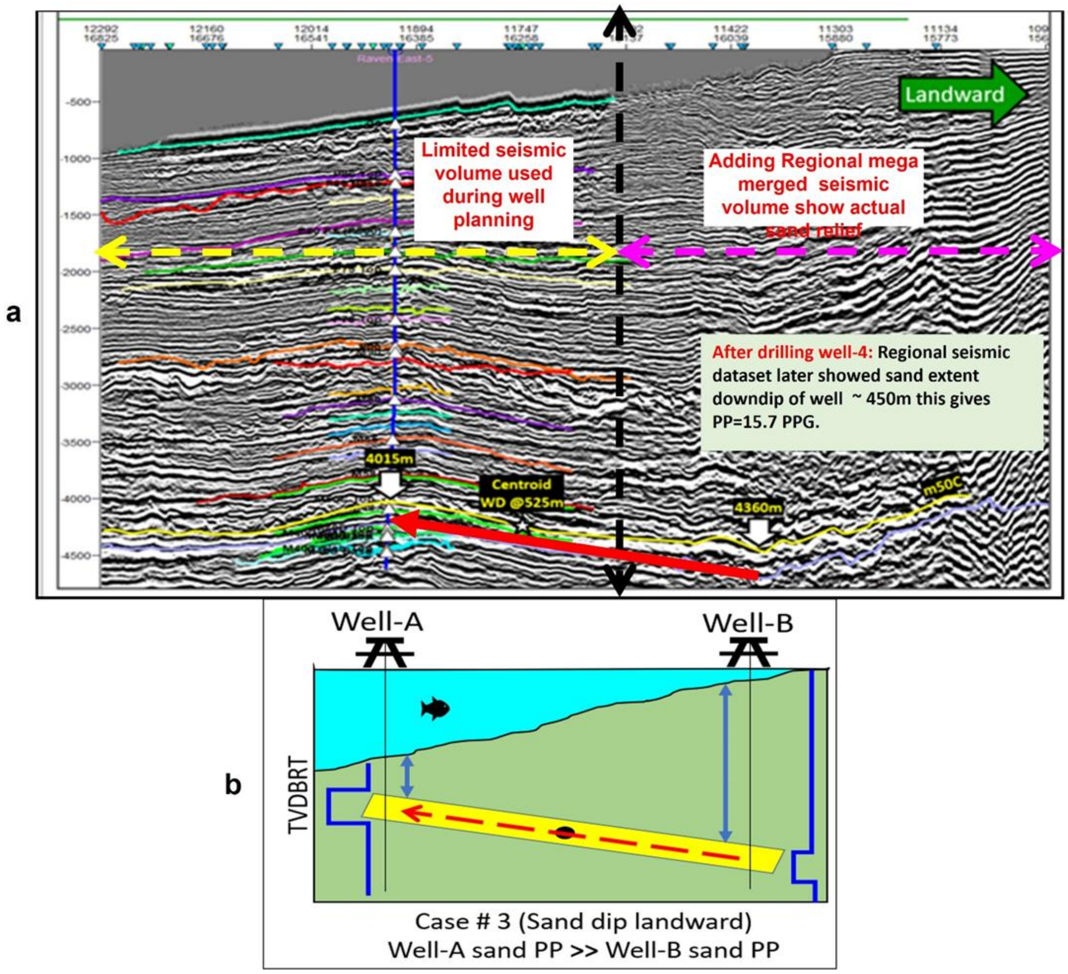


**Fig. 9. (a) Seismic cross section divided vertically by dashed black line showing difference between limited seismic volume used while planning giving shorter relief and lower lateral transfer PP (left of dashed line) compared to mega merged one (right of dashed line). (b) Cartoon of overburden effect on lateral transfer overpressure as sand dip landward impact higher PP compared to seaward one.**

### 4.3 Overpressure mechanism

Seismic mapping shows that there are different structural reliefs along the isolated sand channels (Influx Sand-1 and sand-2), which is the likely reason for pore pressure transfer from down-dip to up-dip. The development nature of the well planning of studied wells led to the use of a local, limited-extent seismic dataset to estimate sand relief. This study observed that predrill small relief around 300 m was estimated while planning, which led to a lower estimated sand pore pressure of <=15.2 ppg EMWT (Fig.9a). After drilling while investigating the influx, the mega-merged regional seismic volume was used to map the sand relief, giving a relief of 450 m for lateral transfer and an estimated pore pressure of 15.5-15.7 ppg. These values are close to the influx and measured pore pressure magnitude at problematic depth 4050 m TVDSS. This study observed that well logs show clear heterogeneity of sand quality and thickness along the studied wells, masking reality of clean sand occurrences as shown in (Fig.9). The observed two isolated sandstone channels caused influxes as they connected to different downdip relief, giving different pore pressure magnitudes.

The planning of development wells was biased to the data collected from exploratory wells drilled 13 years earlier, which did not have any problems at the same stratigraphic level. 3D seismic attribute maps along the likely connected sand channels identified two different isolated sand channels. Well-1 penetrated sand-1 deposits in a silty/shaly marginal area, Well-2 did not penetrate any sand, Well-3 penetrated sand-1 in a good quality sand area and Well-4 penetrated sand-2 deposits in a good quality sand area as shown in (Fig.10). All studied wells had influxes at different EMWT values ranging from 15.5-15.71 ppg at almost the same depth, except well-4 that had influx from Sand-2. This means that they all have different overpressures and are not connected to each other.

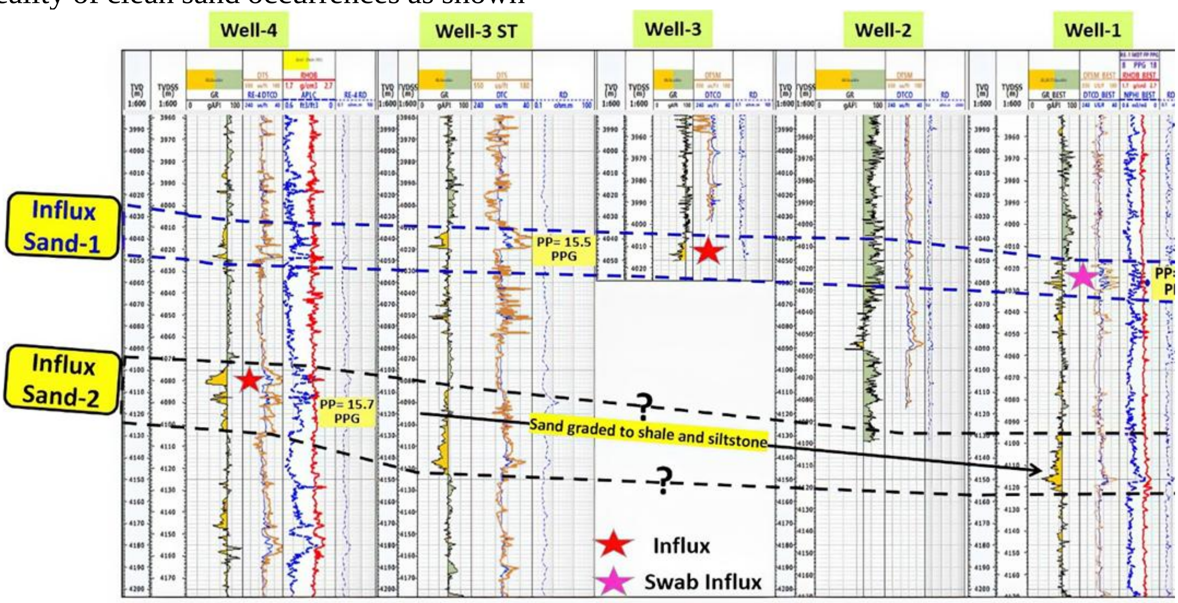


**Fig.10. Correlation of four well logs as quality of influx sand-1 and sand-2 tends to be better toward Well-3 and Well-4 compared to Well-1 and very bad quality in Well-2, this is aligned with kick events red stars.**

## 5. Discussion

Lateral transfer over pressure mechanism can result in kicks/influxes if the effect is not factored in pre-drill planning or during execution. It poses a particular risk during operations because pore pressure monitoring techniques estimate shale pressure, and centroids are caused by sand/silt pressure, which cannot be estimated with petrophysical methods. This study managed to investigate the main problem and introduce new practical workflow and methodology to avoid this problem, either for well planning or drilling pore pressure. Sandstone dipping geometries play a key role for lateral transfer over pressure severity, as sand relief may extend toward shallower or deeper water depth. Results show that sandstone dipping to shallower water (higher overburden stress) create much higher lateral transfer over pressure, compared to those dipping to deeper water (lower overburden stress) (Fig.11).

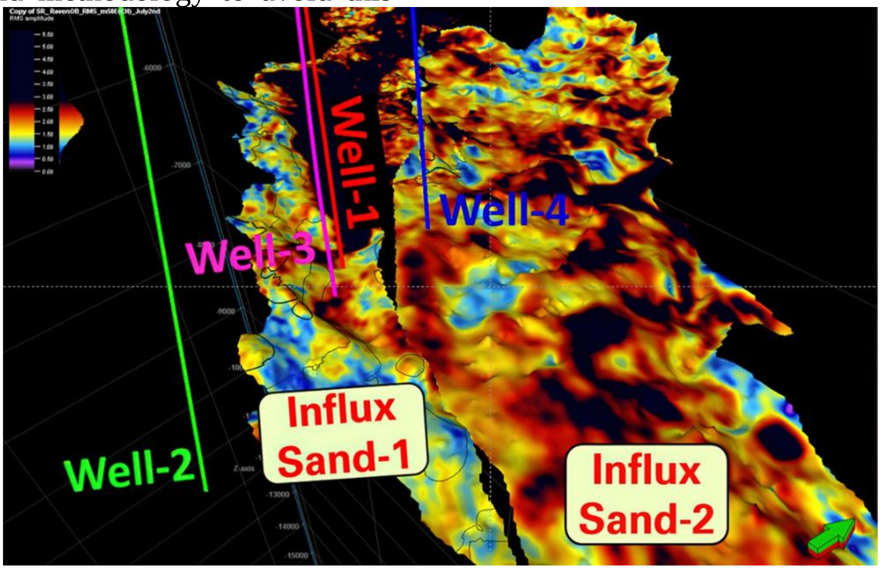


**Fig. 11. 3D seismic attribute map at top problematic sand (Serravallian) showing clear sand channel system called sand-1 and sand-2.**

Previous predrill pore pressure studies and working hypotheses were limited to small scale seismic volume and biased by not including offset wells results. To plan for new development wells in the studied field, pore pressure practitioners should be able to predict pressure of sand bodies that are expected to be penetrated at each development well, based on its structural position against centroids and apparent thicknesses. These findings will help to avoid kicks or influxes and minimize uncertainty window for any future work. Pore pressure practitioners better follow study workflow to avoid missing lateral transfer (centroid) sand overpressure. Accurate estimation of shale pore pressure is a key factor to calculate lateral transfer pressure of dipping sand underline shale. The best shale pore pressure derived from compressional sonic logs that acquired over 4 studied wells, and there is good match observed (Fig.12). Shale PP increased up to 15.1 ppg at base Serravallian problematic zone at +/-4000m tvdbrt, then took very gentle PP regression +/- from 15.2 ppg down to 14.9 ppg at 4500 m tvdbrt. Only well-1 and well-4 show a slight softer trend as go deeper.

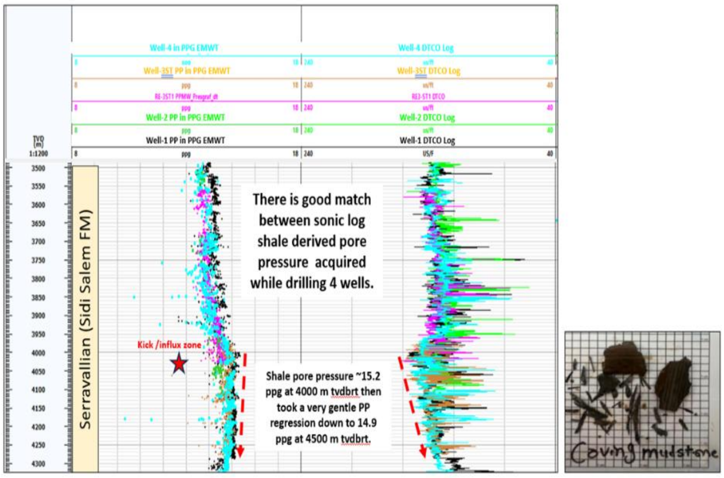


**Fig. 12. Best shale pore pressure derived from compressional sonic logs that acquired over 4 studied wells and there is good match observed.**

Seismic data are usually contaminated with random and coherent noise. This noise prevents the accurate imaging of seismic sections and leads to mistakes in their interpretations (H. et al, 2023). In this study, two types of pre-stack depth migration (PSDM) seismic interval velocities were used to calculate pore pressure then compared to both sonic and resistivity derived pore pressure. Integration of all results gave reliable details for pore pressure prediction Eaton pressure transform method integrated with BP internal Presgraf pressure transform method. Interval seismic velocity profiles were extracted every 1 m along the 4 proposed well locations from both the TTI and FWI seismic velocities. This study confirmed that seismic (1D or 3D cube) velocity transforms is giving low pore pressure compared to the log transform, so authors believe it is a matter of fine tuning the transform parameters (a slightly slower normal trendline overall will bring the velocity-based pressure down). As for the smoothness, well that is typical of seismic velocities generated from travel time information using tomography and even FWI – the seismic velocities are never going to give you the same resolution as the sonic – but that's OK, for regional shale pressure, we don't need all that detail. The regional variations are interesting and tell us something real about how pressure is changing across the study area. By plotting the interval velocity profiles in on a normal scale versus the true vertical depth (TVD) in correlation with logs derived pore pressure. Observed clear decrease of seismic velocity (named seismic anomaly - 4) at problematic zone of base Serravallian sand 4050-4090m tvdbrt, which is equivalent to logs overpressure zone-5 (Fig. 13).

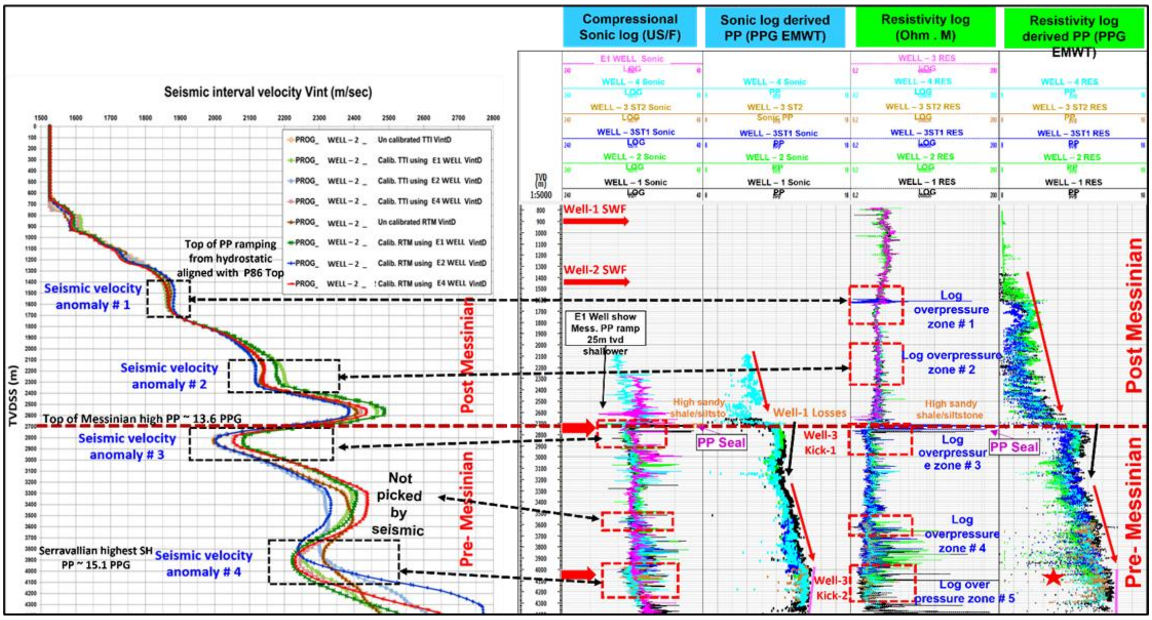


**Fig. 13. Comparison between seismic interval velocity versus logs derived pore pressure, showing good match of seismic anomaly #4 and logs overpressure zone# 5 at problematic zone**

Furthermore, the study observed that seismic derived pore pressure slightly lower (~ 0.5 ppg emwt lower) than logs derived pore pressure. Sonic log pore pressure is much better than resistivity as it affected by salinity and lithology variations compared to sonic. This study confirmed that sand over pressure (above normal pressure) is different magnitude of 4642, 4881 and 5152 psi for problematic sand at 4023, 4020 and 4080 m TVD versus Well-1, Well-3, and Well-4 respectively as per histogram (Fig. 14). These results ensured that Well 1 and 3 penetrated kick sand-1 but Well-4 penetrated kick sand-2. Furthermore, heterogeneous sand quality, thickness and relief within very short distance and limitation of conventional seismic methods to detect such thin sand (3-7 meter) and its extension (Relief) along wells.

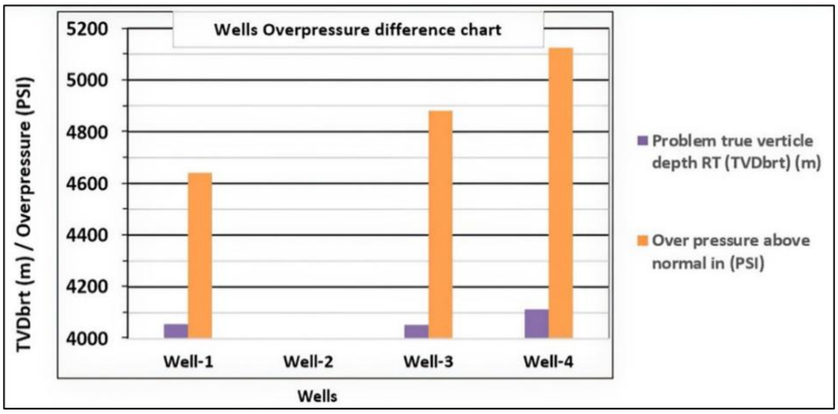


**Fig. 14. sand over pressure histogram showing different magnitude of 4642, 4881 and 5152 psi for problematic sand at 4023, 4020 and 4080 m TVD versus Well-1, Well-3 and Well-4 respectively.**

This study findings and recommendations to minimize nonproductive time are summarized as follows:

1. It is better to use a seismic line that covers the entire sand extent from up-dip to downdip, either from 2D or 3D seismic volume. The lesson learned that limited extension seismic volume that does not cover the full sand extent will lower estimate sand pore pressure accordingly.
2. It is better to create amplitude maps along likely connected sand in depth below the seabed (mudline) to consider maximum relief.
3. Seismic velocity derived pore pressure is slightly lower than sonic one, however it is accepted for regional work but also critical for lateral transfer pressure estimations.
4. The lateral transfer PP estimate must be calculated in depth below mudline or be corrected for changes in water depth at centroid depth compared to the well location, either toward offshore or onshore.
5. Estimations of shale pore pressure will directly impact lateral transfer PP estimates.
6. Do not ignore lateral transfer PP risk in well planning for very thin sand intervals, despite close offset well control, if sands may not be laterally connected to offsets.
7. It is good practice to highlight the expected sand PP more than shale PP to the pore pressure detection specialist before drilling to ensure there is awareness of the potential to encounter sand pressure over and above shale PP.
8. Real time pressure detection practitioners rely mainly on common log-derived pressure trends for shales; therefore, it may be difficult to detect sand pressures above the shale trend.

## 6. Conclusion

- This study highlighted how lateral transfer overpressure can badly affect our ability to use offset wells as direct analogues and importance to map sand relief accurately using regional seismic volumes not limited biased ones.
- Not all centroids are created equal, results show that sands dipping to shallower water (higher overburden stress) create much higher centroid pressure.
- It has proven to be incredibly difficult to forecast sand pressures based on offset well analogues alone, no matter that offset wells are within 400-900 m of the planned well location and drilled from the same manifold as some sands are sub-seismic resolution in thickness.
- When the sands are connected, the overpressure would be the same. However, each individual sand body can be trending in a different orientation and be connected to a different source/extent of overpressure, and so it is important to map every single sand in three dimensions.
- The high pressure in the base Serravallian sand originates from lateral transfer resulting from different structural reliefs along non- connected thin channels. Each well appears to have intersected a different structural compartment of the same sand system, but due to the different relief in each compartment, the overpressure varied.
- Good quality sand encountered in Well-3 and Well-4 may have promoted the influxes compared to Well -1, when underbalance conditions were reached.

**Acknowledgment**

The authors express their sincere appreciation to BP, Wintershall Dea and EGAS, the West Nile Delta partners, for giving approval to publish this technical presentation. Big thank you to my supervisors and my colleagues Juliette Buis-Wegerif and Amal Vittachi. Special acknowledgement to both of Dr Hatem Farouk and Dr. Amir Ismail for their help to review this research. The whole team tried to highlight the importance of our topic to minimize non-productive time for better PPFG well planning and execution to global oil and gas industry.

**References**

Abdel Aal, A., Price, R.J., Vaitl, J.D and Shrallow, J.A., 1994, Tectonic evaluation of the Nile Delta, its impact on sedimentation and hydrocarbon potential, EGPC. 12th Petrl. Expl. Prod. Conf., vol.1, p.19-34.

Argyriadis, I., Graciansky, P.C., Marcoux, J., and Ricou, L.E., 1980, The opening of the Mesozoic Tethys between Eurasia and Arabia-Africa: Mem. du Bureau de Recherché Geologies' et Manières, no.115, p. 199-214.

Athy, L.F. 1930. Density, porosity and compaction of sedimentary rocks. In AAPG Bulletin 14(1): 1–24.

Babu S, Sircar A (2011) A comparative study of predicted and actual pore pressures in Tripura, India. J Petrol Technol Altern Fuels 2(9):150–160.

Bowers, G.L., "Pore Pressure Estimation from Velocity Data: Accounting for Overpressure Mechanisms Besides Under compaction" IADC/SPE paper No. 27488, Feb.1994.

Das T, Soumyajit M (2020) Pore pressure determination methods. In: Das T, Mukherjee S (eds) Sediment compaction and applications in petroleum geoscience. Springer, Switzerland, pp 27–29. https:// doi. org/ 10. 1007/978-3- 030- 13442-6_3

Dutta, N. C. 1987. Geopressure. Tulsa: Society of Exploration Geophysicists.

Eaton, B.A. 1975. The Equation for Geopressure Prediction from Well Logs. 50th Annual Fall Meeting of The Society of Petroleum Engineers of AIME, Dallas, Texas, Sept 28 – Oct 1, 1975. SPE-5544-MS http://dx.doi.org/10.2118/5544-MS.

Heppard PD, Albertin M (1998) Abstract: abnormal pressure evaluation of the recent Pliocene and Miocene gas discoveries from the eastern Nile Delta, Egypt, using 2D and 3D seismic Data. AAPG Houston Geol Soc Bull 41(3):16–17.

Heppard, P.D., and Traugott, M. 1998. Use Of Seal, Structural, and Centroid Information in Pore Pressure Prediction. Presented at the American Association of Drilling Engineers Forum on Pressure Regimes in Sedimentary Basins and Their Prediction, Houston, Texas, Sept 2-4, 1998.

Hottman, C.E. and Johnson, R.K. 1965. Estimation of Formation Pressures from Log-derived Shale Properties. J Pet Technol 16(6): 717–722.

Ismail, A., Ewida, H.F., Nazeri, S., Al-Ibiary, M.G. and Zollo, A., 2022. Gas channels and chimneys prediction using artificial neural networks and multi-seismic attributes, offshore West Nile Delta, Egypt. Journal of Petroleum Science and Engineering, 208, p.109349.

Ismail, A., Ewida, H.F., Al-Ibiary, M.G., Nazeri, S., Salama, N.S., Gammaldi, S. and Zollo, A., 2021. The detection of deep seafloor pockmarks, gas chimneys, and associated features with seafloor seeps using seismic attributes in the West offshore Nile Delta, Egypt. Exploration Geophysics, 52(4), pp.388-408.

Kellner A, Brink G, El-Khawaga H (2018) Depositional history of the western Nile Delta, Egypt: Late Rupelian to Pleistocene. AAPG Bull 102(09):1841–1865. https://doi.org/10.1306/02161817234

Maha K, Nasser A, Abdel-khalek E (2022) Pre-drill pore pressure prediction from 1D seismic velocity profile to 3D modeling using high resolution full waveform inversion velocity (FWI): deep water offshore, West Nile Delta. Geomech.

Geophys. Geo-energ. Geo-resour. (2022) 8:213
Monir, M. and Shenkar, O., 2017. Pre-Messinian petroleum system and trapping style, offshore western Nile Delta, Egypt. In AAPG/SPE Africa Energy and Technology Conference (pp. 5-7).
Mouchet, J. and Mitchell, A., 1989. Abnormal Pressure While Drilling. Boussens: Elf Aquitane.
Neev, D., 1975, Tectonic evolution of the Middle East and the Levantine basin (easternmost Mediterranean): Geology, no.3, pp. 683-686.
Osborne, M.J. and Swarbrick, R.E., 1997. Mechanisms for Generating Overpressure in Sedimentary Basins: A Re-evaluation. AAPG Bulletin 81:1023–1041.
Rubey, W. W., and Hubbert M.K., 1959. Role of fluid pressure in mechanics of overthrust faulting. II. Overthrust belt in geosyncline area of western Wyoming in light of fluid-pressure hypothesis. Geological Society America Bulletin, 70(2):167–206.
Saleh MH (2018) Introduction. Chap. 1 in MSc. Thesis: the structural geometries and geological evolution of the detachment plio-pliestocene fault systems of the eastern Nile Delt, Egypt, by M. H. Saleh, Cairo, p 22.

Staff, Offshore (2019) BP brings two more gas fields onstream offshore northern Egypt: BP has produced first gas from two more fields in the West Nile Delta concession in the Mediterranean Sea off Egypt. Feb 11. Accessed 11 Nov 2021. https:// www. offshore- mag. com/ field-development/ artic le/ 16791 052/ bp-brings- two more-gas- fields- onstream-offshore- north ern- egypt
Sundaram KM, Rita J (2008) Eaton's equation and compaction—a study. In: 7th International conference and exposition on petroleum geophysics, pp 311–317. https://www. spgin dia. org/ 2008/ 311. pdf
Traugott, M.O., 1997. Pore Pressure and Fracture Pressure Determinations in Deepwater. In Deepwater Technology (Supplement to World Oil & Pipeline & Gas Industry), 68 –70. Houston: Gulf Publishing Company.
Wallace, W.E. 1965. Application of Electric Log Measured Pressure to Drilling Problems and A New Simplified Chart for Wellsite Pressure Computation. The Log Analyst, 6:4 –10.
Yardley, G.S. and Swarbrick, R.E. 2000. Lateral Transfer: A Source of Additional Overpressure? Marine and Petroleum Geology 17, 523–53.